Title: Maximizing the impact of limited vaccine supply under different epidemic conditions: a two-city monkeypox modelling analysis

Authors: Jesse Knight[1,2], Darrell H.S. Tan[1,2,3,4], and Sharmistha Mishra[1,2,3,4]

[1]MAP Centre for Urban Health Solutions, Unity Health Toronto
[2]Institute of Medical Science, University of Toronto
[3]Institute of Health Policy, Management, and Evaluation, University of Toronto
[4]Division of Infectious Diseases, Department of Medicine, University of Toronto

Journal: preprint

Date: 2022 Aug 18

Abstract

BACKGROUND. In the current global monkeypox outbreak, many jurisdictions have been faced with limited vaccine supply, motivating interest in efficient allocation. We sought to explore optimal vaccine allocation between two linked transmission networks over a short-term time horizon, across a range of epidemic conditions. METHODS. We constructed a deterministic compartmental SVEIR model of monkeypox transmission. We parameterized the model to reflect two representative, weakly connected GBMSM sexual networks (cities) in Ontario. We simulated roll-out of 5000 vaccine doses over 15 days, starting 60 days after epidemic seeding by 10 imported cases. Within this model, we varied: the relative city (network) sizes, epidemic potentials (R_0), between-city mixing, and distribution of imported/seed cases between cities. In each context (combination of varied factors), we then identified the "optimal" allocation of doses between cities — resulting in the fewest infections overall by day 120. RESULTS. Under our modelling assumptions, we found that a fixed supply of vaccines could generally avert more infections over short-term time horizons when prioritized to: a larger transmission network, a network with more initial infections, and a network with greater R_0. Greater between-city mixing decreased the influence of initial seed cases, and increased the influence of city R_0 on optimal allocation. Under mixed conditions (e.g. fewer seed cases but greater R_0), optimal allocation saw doses shared between cities, suggesting that proximity-based and risk-based vaccine prioritization can work in combination to minimize transmission. INTERPRETATION. Prioritization of limited vaccine supply based on network-level risk factors can help minimize transmission during an emerging epidemic. Such prioritization should be grounded in an understanding of context-specific drivers of risk, and should acknowledge the potential connectedness of multiple transmission networks.

1 Introduction

The emerging outbreak of monkeypox virus (MPVX) worldwide includes 1,112 cases in Canada as of 2022 August 17 [1]. A third-generation replication-deficient smallpox vaccine (Imvamune®) has been licensed for use against monkeypox and related orthopoxviruses in Canada since 2020, for the purpose of national security [2]. Shortly after local cases were reported, rapid pre-exposure prophylaxis vaccination efforts were initiated to help reduce acquisition, infectivity, and/or disease severity among communities disproportionately affected by MPVX, including gay, bisexual, and other men who have sex with men (GBMSM) [3]. However, many jurisdictions, across countries and within Canada, were faced with a limited local supply of vaccines during the first few weeks of MPVX outbreak.

It is well-established that prioritizing a limited supply of vaccines to sub-populations experiencing disproportionately higher risk — individual-level and/or network-level acquisition and/or transmission risk — can maximize infections averted [4,5]. Such networks may have different characteristics that shape the epidemic potential (R_0) within the network itself. A network's connectedness to other networks further shapes the chances and number of imported cases by the time vaccine allocation decisions and roll-out begin.

We sought to explore optimal allocation of a fixed supply of MPVX vaccine across two jurisdictions — i.e. weakly connected transmission networks — under different epidemic conditions. Specifically, we explored differences between two jurisdictions in: population size of GBMSM; epidemic potential (R_0); imported/seed cases; and connectedness of the two jurisdictions. The goal of this modeling study was to produce fundamental and generalizable insights into MPVX vaccine prioritization in the context of interconnected sexual networks, using jurisdictions (cities) within a province like Ontario, Canada as an example.

2 Methods

We constructed a deterministic compartmental SVEIR (susceptible, vaccinated, exposed, infectious, recovered) model of MPVX transmission. The modelled population aimed to represent the Ontario GBMSM community, and included two levels of sexual risk (higher, lower) and two weakly connected transmission networks (cities A, B). Figure 1a illustrates the modelled city/risk strata, Figure 1b illustrates the SVEIR health states, and Table 1 summarizes the default model parameters. To parameterize the model, we drew on prior analyses of GBMSM sexual networks in Canada [6,7], and emerging MPVX epidemiological data in the context of the current epidemic [8–12]. Appendix A provides additional details about the model implementation and parameterization.

We initialized all model runs with 10 imported/seed cases, distributed across the exposed and infectious stages proportionally by mean stage duration. We then simulated distribution of 5000 vaccine doses over 15 days, 60 days after initial cases were imported (though not necessarily detected). Doses were imperfectly prioritized to the higher risk group with 90% sensitivity — i.e. 4500 doses reach the higher risk group and 500 each the low risk group, reflecting early risk-based eligibility criteria in some jurisdictions [3].

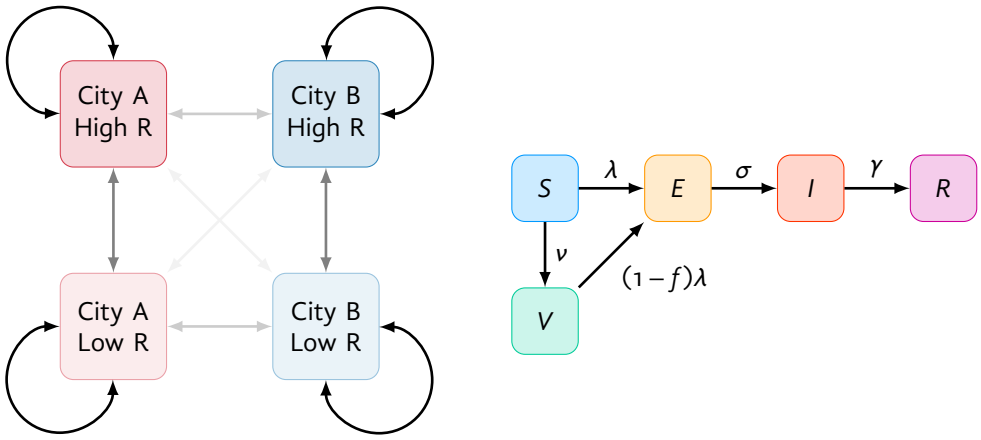

(a) Cities, risk groups, and contact networks (b) Health states and transitions

Figure 1: Model structure

(a) High/Low R: risk groups; arrow opacity is proportional to contact network connectivity between groups. (b) *S*: susceptible; *V*: vaccinated; *E*: exposed; *I*: infectious; *R*: recovered. See Table A.1 and Appendix A for rate definitions.

Using this model, we explored optimal vaccine allocation between cities A and B over a range of epidemic conditions. For a given set of conditions, we defined the optimal vaccine allocation as that which resulted in the fewest cumulative infections by day 120 in both cities.[1]

We chose this 60-day time horizon and fixed 5000 vaccine doses to reflect a plausible medium-term optimization problem relevant to the early MPVX situation in Ontario. In reality, multiple changing time horizons may require consideration, different numbers of doses may become available, and different rates of vaccination may be possible. We aimed to obtain generalizable insights about the relationships between specific epidemic conditions and efficient geographic prioritization of vaccines during an outbreak.

As one specific example setting, we chose parameters representative of Toronto (city A) and another medium-sized Ontario city (city B), with GBMSM population sizes of 80,000 and 20,000, respectively, and 10% sexual/social network connectivity ($\epsilon_c = 0.9$) [7]. We also modelled $R_0 = 2.0$ in Toronto versus 1.5 in city B, reflecting differences in sexual network density as suggested by differential prevalence of bacterial sexually transmitted infections across Ontario cities [19,20]. Finally, we simulated 100% imported/seed cases in Toronto, reflecting early MPVX case distribution in Ontario [17]. We then compared two strategies of vaccine allocation by city: (a) proportional to population size; and (b) "optimal" (fewest infections by day 120).

Next, we performed a "grid sweep" of the following epidemic conditions, and identified the optimal vaccine allocation between cities A and B for each combination of conditions:

[1] Optimal allocation was identified using the `optimize` function in R.

Table 1: Model parameters, including default values and ranges explored via grid sweep

Parameter	Stratum	Value	Range	Ref
Population size	overall	100,000		[6][a]
	fraction in city A	.50	[.20, .80]	[a]
Fraction higher risk	city A	.10	[.01, .50][b]	[6][a]
	city B	.10		[6][a]
Contact rate	close non-sexual, all	1		[a]
	sexual, low risk	.01		[6][a]
	sexual, high risk, city A	.178[c]	[.10, .25][b]	[6,13][a]
	sexual, high risk, city B	.178[c]		[6,13][a]
Assortativity	cities, all contacts	.90	[.70, 1.0]	[7][a]
	risk, close non-sexual	0		[a]
	risk, sexual	.50		[a]
Per-contact SAR	close non-sexual	.05		[14]
	sexual	.90[c]		[13][a]
Initial infections	overall	10		[a]
	fraction in city A	.50	[0.0, 1.0]	[a]
Duration of period	latent/incubation	7		[10–12]
	infectious/symptoms	21		[9,10]
Fraction isolated among infected		.50		[10][a]
Vaccines available		5000		[a]
Vaccine effectiveness[d]		.85		[2,15,16]
Vaccine prioritization sensitivity	high risk	.90		[3][a]
Vaccine allocation	city A	.50	[0.0, 1.0][e]	—

All durations in days; all rates in per-day. SAR: secondary attack rate. [a] Assumed / representative. [b] Calculated to fit $R_0 \in [1, 2]$. [c] Calculated to fit $R_0 = 1.5$, reflecting pre-vaccination estimate of MPVX R_0 in Ontario [17] via [18]. [d] Leaky-type. [e] Optimized parameter.

- relative size of city A versus B (1/4 to 4 times)
- relative epidemic potential in city A (R_0 in city A from 1 to 2, versus fixed 1.5 in city B),[2] adjusted via the sexual activity of the higher risk group in the city A
- between-city mixing (0 to 30% of all contacts formed randomly between cities)
- fraction of imported/seed cases in city A versus B (0–100%)

3 Results

Figure 2 illustrates modelled monkeypox incidence and cumulative infections in "Toronto" versus city B under different vaccine allocation strategies. Due to the larger population size, greater epidemic potential (R_0), and having all imported/seed cases in Toronto in this scenario, allocating all 5000 vaccine doses to Toronto yielded the fewest infections by day 120: 1630 (c). Allocating vaccines proportionally to city size (b) yielded 1956 infections, while no vaccination (a) yielded 3466 infections.

As shown in Figure 2c, allocating most/all doses to one city (A) allows incidence to rise exponentially in the other city (B). However, this approach can still avert more infections overall over shorter time horizons, after which more doses may become available. Figure B.1 illustrates the opposite case (default model parameters in Table 1): two identical cities with equal seeding, where the optimal allocation is, unsurprisingly, equal between cities.

Figure 3 illustrates optimal vaccine allocation between cities A and B across different epidemic conditions. Figures B.2–B.5 further illustrate the absolute and relative numbers of infections averted under optimal allocation versus no vaccination (B.2–B.3), and versus vaccine allocation proportional to city size (B.4–B.5). Thus, Figures B.2–B.5 show under what conditions optimal allocation is most important.

The strongest determinants of optimal vaccine allocation were: relative epidemic potential (R_0), share of seed cases, and city size; though city size was proportional to the size of the higher risk group under our modelling assumptions. Thus, if a larger city had large R_0 and the majority of seed cases, it was best to allocate most/all doses to that city in our analysis (solid red/blue corners in Figure 3).

For smaller cities with large R_0 and the majority of seed cases, it was sometimes possible to vaccinate the entire higher risk group; in this case, the remaining doses were best allocated to the higher risk group in the other city, yielding the plateaus (solid yellow triangles) in Figure 3: (a,d,g) upper right; (c,f,i) lower left. This plateau highlights how priority populations can change if/after high levels of coverage are achieved in other populations.

When cities with most/all seed cases had smaller R_0, optimal allocation saw doses shared between cities (to varying degrees), suggesting that both risk-based (reflecting R_0) and proximity-based (reflecting initial cases) prioritization strategies worked together to minimize transmission. In such cases, the other city necessarily had few/no seed cases but larger R_0, to which the same findings apply. These conditions are represented by the yellow diagonal segments in all facets of Figure 3.

[2] City-specific R_0 calculated assuming no inter-city mixing.

Finally, increased levels of mixing between cities mainly acted to reduce the influence of initial seed cases, and increase the influence of R_0 on optimal allocation of vaccines to each city; this finding is visible in Figure 3 as stronger vertical gradients (contours are relatively more horizontal) in (a,b,c) with more inter-city mixing, versus stronger horizontal gradients (contours are relatively more vertical) in (g,h,i) with less inter-city mixing.

4 Interpretation

We sought to explore how different epidemic conditions could affect optimal allocation of a fixed supply of monkeypox virus (MPVX) vaccine across two weakly connected transmission networks (e.g. cities or jurisdictions). Under our modelling assumptions, we found that: vaccines could generally avert more infections when prioritized to a larger network, a network with more initial infections, and a network with greater epidemic potential (R_0).

Although our study, for simplicity, focused on two weakly-connected networks, it highlights the importance of measuring outcomes for a population overall, by considering that geographies are comprised of interconnected networks. That is, while cities across Canada, and globally, feature important within- and between-city differences in size and configuration of transmission networks [21,22], and in access to interventions/services [20,23,24], ultimately these cities remain connected with respect to transmission, and cannot be considered in isolation over longer time horizons [7,22,25].

Within such interconnected settings, our findings are consistent with previous studies which show that prioritizing limited vaccine supply/resources to communities or settings with the highest epidemic potential (shaped by density and other features of the contact network) generally yields the greatest benefit for the population overall [4,5,26]. We also identified how key factors, such as number of imported cases and connections between networks, shape efficient early vaccine roll-out. While our model parameterization reflected GBMSM sexual networks in Ontario, our findings have wider implications for vaccine roll-out globally. The persistent absence of vaccine supply and roll-out in regions already endemic for MPVX outbreaks across West and Central Africa, including (although not yet reported) in the context of GBMSM and sexual minorities, poses the largest threat to the control and mitigation of MPVX globally [27], paralleling missed opportunities in achieving COVID-19 vaccine equity [28].

Prioritizing based on risk also requires understanding risk. Early vaccine roll-out in Ontario reached Toronto, where cases were already detected, the population size was large, and rates of bacterial sexually transmitted infections suggested a potentially denser sexual network and thus, greater epidemic potential [13]. Our model implemented differential R_0 between cities via contact rates; however, epidemic potential may also be linked to intervention access, including access to diagnoses and isolation support [23,29]. Thus, our findings signal the importance of characterizing the drivers of epidemic potential across jurisdictions and communities, including participatory, community-based surveillance and research into the contexts that lead to disproportionate risks at a network-level, not just an individual-level [30,31].

Our study aimed to provide fundamental and generalizable findings, and thus explored a broad sensitivity analysis to identify conditions that can shape optimal short-term vaccine allocation, with very limited supply. One limitation of our study is that we used a simple compartmental model, with only two risk groups; future work would benefit from more nuanced

representations of risk, for example, using individual-based sexual network models. Second, our study only examined two transmission networks ("cities"); incorporation of additional networks could yield more interesting prioritization findings. However, we expect that the general principles and insights from two networks would apply across multiple networks.

Conclusion [TODO]

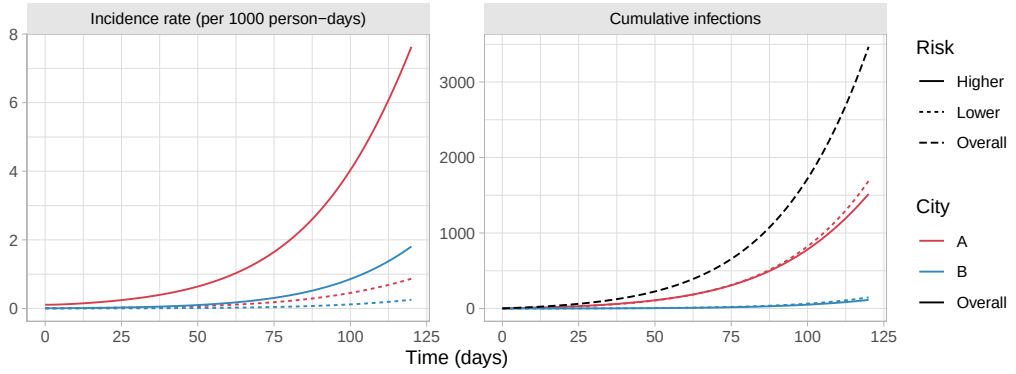

(a) No vaccination

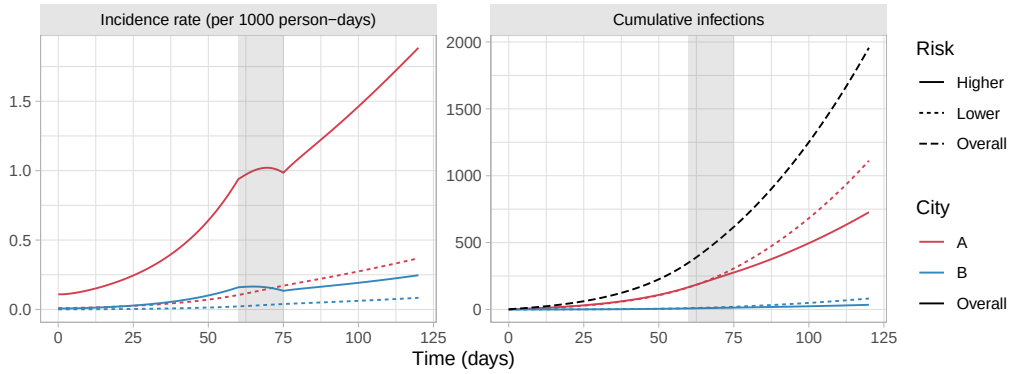

(b) Proportional to city size: 75% city A, and 25% city B

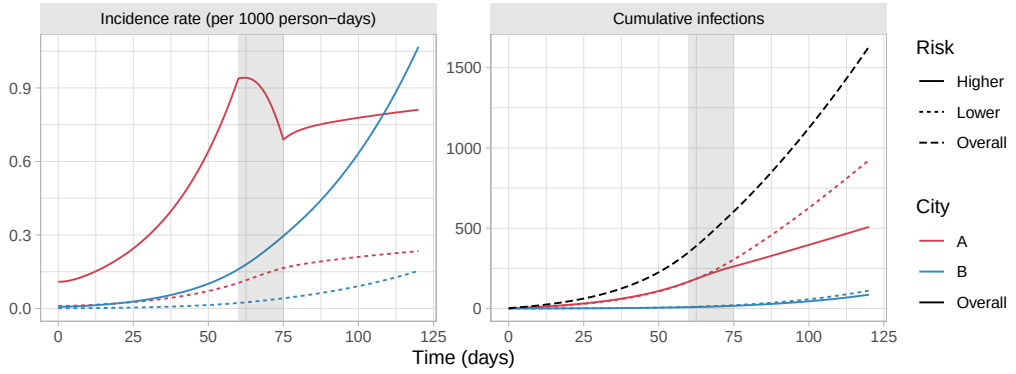

(c) Optimal (most infections averted by day 120): 100% city A

Figure 2: Modelled monkeypox incidence and cumulative infections in two cities under two different vaccine allocation scenarios

Gray bar indicates period of vaccine roll-out (days 60–75). Cities loosely reflect Toronto and another medium-sized Ontario city.

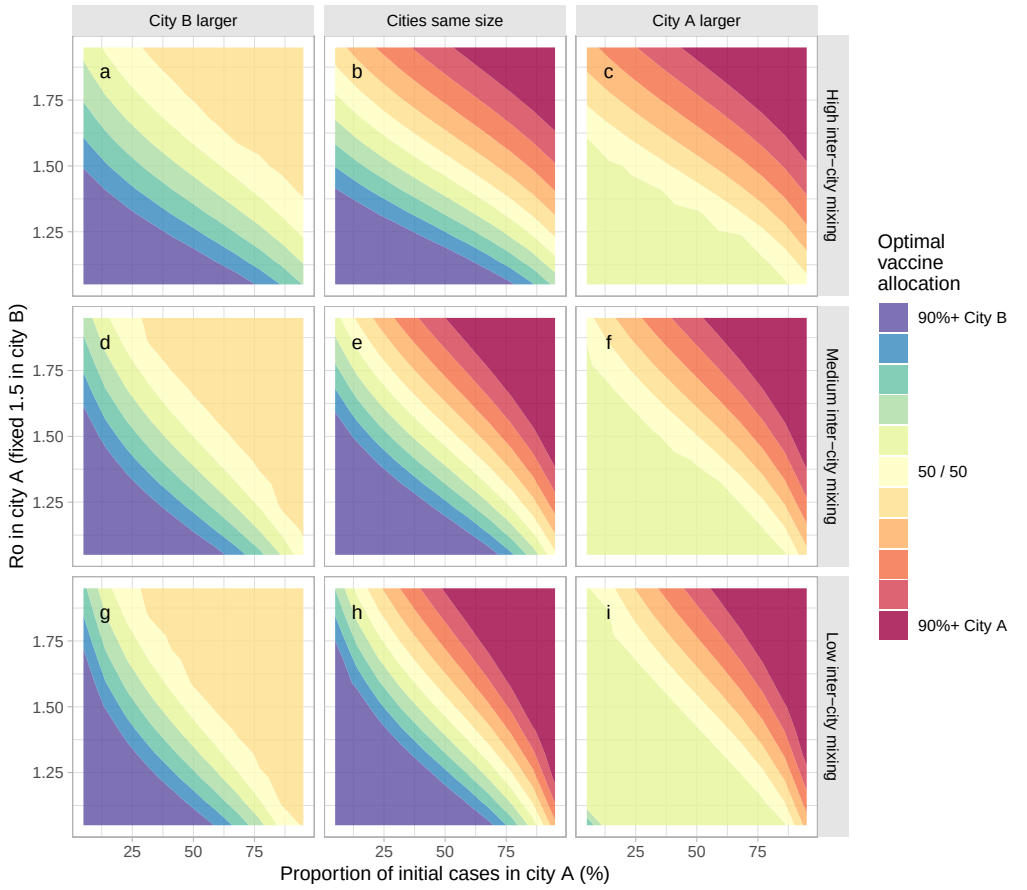

Figure 3: Optimal vaccine allocation between two cities under different epidemic conditions

R_0 in city A varies via the sexual activity among the high risk group in city A. Optimal allocation is defined as fewest cumulative infections by day 120. Larger city is 3 times the size of the other city. Most, moderate, and least inter-city mixing use $\epsilon_c = \{0.8, 0.9, 0.95\}$, respectively.

References

[1] Public Health Agency of Canada. *Monkeypox epidemiology update*. Aug. 2022. URL: https://health-infobase.canada.ca/monkeypox/.

[2] Public Health Agency of Canada. *Interim guidance on the use of Imvamune in the context of monkeypox outbreaks in Canada*. June 2022. URL: https://www.canada.ca/content/dam/phac-aspc/documents/services/immunization/national-advisory-committee-on-immunization-naci/guidance-imvamune-monkeypox/guidance-imvamune-monkeypox-en.pdf.

[3] Toronto Public Health. *Monkeypox Vaccine Fact Sheet*. Aug. 2022. URL: https://www.toronto.ca/wp-content/uploads/2022/07/97ef-MonkeypoxVaccineFactSheet.pdf.

[4] Geoffrey Garnett. "Role of herd immunity in determining the effect of vaccines against sexually transmitted disease". In: *Journal of Infectious Diseases* 191.S1 (Jan. 2005). URL: https://doi.org/10.1086/425271.

[5] Sharmistha Mishra et al. "A Vaccination Strategy for Ontario COVID-19 Hotspots and Essential Workers". In: *Science Briefs of the Ontario COVID-19 Science Advisory Table* 2.26 (2021). URL: https://doi.org/10.47326/ocsat.2021.02.26.1.0.

[6] Linwei Wang et al. "Mathematical modelling of the influence of serosorting on the population-level HIV transmission impact of pre-exposure prophylaxis". In: *AIDS* 35.7 (June 2021), pp. 1113–1125. URL: http://www.doi.org/10.1097/QAD.0000000000002826.

[7] Eric Armstrong et al. "Travelling for sex, attending gay-specific venues, and HIV-related sexual risk among men who have sex with men in Ontario, Canada". In: *Canadian Journal of Human Sexuality* 29.3 (Dec. 2020), pp. 380–391. URL: http://www.doi.org/10.3138/CJHS.2019-0054.

[8] Public Health Ontario. *Multi-Jurisdictional Monkeypox Outbreak 2022 – What We Know So Far*. July 2022. URL: https://www.publichealthontario.ca/en/Diseases-and-Conditions/Infectious-Diseases/Vector-Borne-Zoonotic-Diseases/Monkeypox.

[9] Hugh Adler et al. "Clinical features and management of human monkeypox: a retrospective observational study in the UK". In: *The Lancet Infectious Diseases* 22.8 (Aug. 2022), pp. 1153–1162. URL: http://www.doi.org/10.1016/s1473-3099(22)00228-6.

[10] John P. Thornhill et al. "Monkeypox Virus Infection in Humans across 16 Countries - April-June 2022". In: *New England Journal of Medicine* (July 2022). URL: https://doi.org/10.1056/NEJMoa2207323.

[11] Kelly Charniga et al. "Estimating the incubation period of monkeypox virus during the 2022 multi-national outbreak". In: *medRxiv* (June 2022). URL: http://www.doi.org/10.1101/2022.06.22.22276713.

[12] Fuminari Miura et al. "Estimated incubation period for monkeypox cases confirmed in the Netherlands, May 2022". In: *Eurosurveillance* 27.24 (June 2022). URL: http://www.doi.org/10.2807/1560-7917.es.2022.27.24.2200448.

[13] Akira Endo et al. "Heavy-tailed sexual contact networks and the epidemiology of monkeypox outbreak in non-endemic regions, May 2022". In: *medRxiv* (June 2022). URL: https://doi.org/10.1101/2022.06.13.22276353.

[14] Ellen M. Beer and V. Bhargavi Rao. "A systematic review of the epidemiology of human monkeypox outbreaks and implications for outbreak strategy". In: *PLOS Neglected Tropical Diseases* 13.10 (2019), e0007791. URL: http://www.doi.org/10.1371/journal.pntd.0007791.

[15] P. E.M. Fine et al. "The transmission potential of monkeypox virus in human populations". In: *International Journal of Epidemiology* 17.3 (Sept. 1988), pp. 643–650. URL: https://doi.org/10.1093/ije/17.3.643.

[16] United States Centers for Disease Control and Prevention. *Monkeypox and Smallpox Vaccine Guidance*. June 2022. URL: https://www.cdc.gov/poxvirus/monkeypox/clinicians/smallpox-vaccine.html.

[17] Public Health Ontario. *Monkeypox in Ontario: May 20, 2022 to August 15, 2022*. Aug. 2022. URL: https://www.publichealthontario.ca/en/Diseases-and-Conditions/Infectious-Diseases/Vector-Borne-Zoonotic-Diseases/Monkeypox.

[18] Sam Abbott et al. *EpiNow2: Estimate Real-Time Case Counts and Time-Varying Epidemiological Parameters*. 2020. URL: http://www.doi.org/10.5281/zenodo.3957489.

[19] Dionne Gesink et al. "Spatial epidemiology of the syphilis epidemic in Toronto, Canada". In: *Sexually Transmitted Diseases* 41.11 (Nov. 2014), pp. 637–648. URL: http://www.doi.org/10.1097/OLQ.0000000000000196.

[20] Trevor A. Hart et al. “Prevalence of HIV and sexually transmitted and blood-borne infections, and related preventive and risk behaviours, among gay, bisexual and other men who have sex with men in Montreal, Toronto and Vancouver: results from the Engage Study”. In: *Canadian Journal of Public Health* 112.6 (Dec. 2021), pp. 1020–1029. URL: https://doi.org/10.17269/s41997-021-00546-z.

[21] Hyman M. Scott et al. “Sexual behavior and network characteristics and their association with bacterial sexually transmitted infections among Black men who have sex with men in the United States”. In: *PLOS ONE* 10.12 (Dec. 2015), e0146025. URL: http://www.doi.org/10.1371/journal.pone.0146025.

[22] Dionne Gesink et al. “Conceptualizing Geosexual Archetypes: Mapping the Sexual Travels and Egocentric Sexual Networks of Gay and Bisexual Men in Toronto, Canada”. In: *Sexually Transmitted Diseases* 45.6 (June 2018), pp. 368–373. URL: http://www.doi.org/10.1097/OLQ.0000000000000752.

[23] Gregorio A. Millett et al. “Comparisons of disparities and risks of HIV infection in black and other men who have sex with men in Canada, UK, and USA: A meta-analysis”. In: *The Lancet* 380.9839 (July 2012), pp. 341–348. URL: http://www.doi.org/10.1016/S0140-6736(12)60899-X.

[24] Jason Doran et al. “An update on the performance of STI services for gay and bisexual men across European cities: Results from the 2017 European MSM Internet Survey”. In: *Sexually Transmitted Infections* 97.3 (May 2021), pp. 201–208. URL: http://www.doi.org/10.1136/sextrans-2020-054681.

[25] Isaac I. Bogoch et al. “Assessment of the potential for international dissemination of Ebola virus via commercial air travel during the 2014 west African outbreak”. In: *The Lancet* 385.9962 (Jan. 2015), pp. 29–35. URL: http://www.doi.org/10.1016/S0140-6736(14)61828-6.

[26] Sarah Jane Anderson et al. “Maximising the effect of combination HIV prevention through prioritisation of the people and places in greatest need: A modelling study”. In: *The Lancet* 384.9939 (July 2014), pp. 249–256. URL: https://doi.org/10.1016/S0140-6736(14)61053-9.

[27] John Zarocostas. “Monkeypox PHEIC decision hoped to spur the world to act”. In: *The Lancet* 400.10349 (July 2022), p. 347. URL: http://www.doi.org/10.1016/S0140-6736(22)01419-2.

[28] Gavin Yamey et al. “It is not too late to achieve global covid-19 vaccine equity”. In: *BMJ* 376 (Mar. 2022). URL: http://www.doi.org/10.1136/bmj-2022-070650.

[29] Muge Cevik et al. “Support for self-isolation is critical in covid-19 response”. In: *BMJ* 372 (Jan. 2021). URL: http://www.doi.org/10.1136/BMJ.N224.

[30] Stefan Baral et al. “Modified social ecological model: A tool to guide the assessment of the risks and risk contexts of HIV epidemics”. In: *BMC Public Health* 13.1 (May 2013), p. 482. URL: https://doi.org/10.1186/1471-2458-13-482.

[31] Muge Cevik and Stefan D. Baral. “Networks of SARS-CoV-2 transmission”. In: *Science* 373.6551 (July 2021), pp. 162–163. URL: https://doi.org/doi/10.1126/science.abg0842.

Funding

The study was supported by: the Natural Sciences and Engineering Research Council of Canada (NSERC CGS-D); and the University of Toronto Emerging and Pandemic Infections Consortium (EPIC) MPXV Collaborative Rapid Research Response.

Acknowledgements

We thank: Kristy Yiu (Unity Health Toronto) for research coordination support; Huiting Ma, Linwei Wang, Oliver Gatalo, and Ekta Mishra (Unity Health Toronto) for support conceptualizing and parameterizing the model; and Mackenzie Hamilton (Unity Health Toronto) for her feedback on the manuscript. We also thank Toronto Public Health and members of the MPox Community Mobilization Group for their insights, ongoing engagement, and feedback on preliminary results.

Contributions

JK and SM conceptualized and designed the study, and drafted the manuscript. JK developed the model, conducted the analyses, and generated the results. DT reviewed the results and contributed to manuscript writing.

Data Availability

All analysis code is available at: `github.com/mishra-lab/mpox-model-compartmental`

APPENDIX

Title: Maximizing the impact of limited vaccine supply under different epidemic conditions: a two-city monkeypox modelling analysis

Authors: Jesse Knight[1,2], Darrell H.S. Tan[1,2,3,4], and Sharmistha Mishra[1,2,3,4]

[1]MAP Centre for Urban Health Solutions, Unity Health Toronto
[2]Institute of Medical Science, University of Toronto
[3]Institute of Health Policy, Management, and Evaluation, University of Toronto
[4]Division of Infectious Diseases, Department of Medicine, University of Toronto

Date: 2022 Aug 18

A Model Details

Table A.1 summarizes the notation used.

Table A.1: Notation

Symbol	Definition
c	city index $\in$ {A, B}
r	risk group index $\in$ {high, low}
y	type of contact index $\in$ {sexual, close non-sexual}
N	population size
C	contact rate
Q	total contacts offered: NC
ϵ	assortativity parameter $\in$ [1: assortative, 0: random]
λ	incidence rate (force of infection)
β	secondary attack rate [a]
σ^{-1}	duration of latent/incubation period
γ^{-1}	duration of infectious/symptom period
Φ	probability of contact formation
ρ	proportion isolating among infectious
ν	vaccination rate
f	vaccine effectiveness (leaky=type)

All durations in days; all rates in per-day. [a] per-partnership transmission probability

A.1 Differential Equations

Equation (A.1) summarizes the system of differential equations for the SVEIR health states; each equation is repeated for each combination of city c (A, B) and risk group r (high, low) (4 total), but we omit the cr index notation for clarity.

$$\frac{d}{dt}S = -\nu S - \lambda S \tag{A.1a}$$

$$\frac{d}{dt}V = +\nu S - (1-f)\lambda V \tag{A.1b}$$

$$\frac{d}{dt}E = +\lambda S + (1-f)\lambda V - \sigma E \tag{A.1c}$$

$$\frac{d}{dt}I = +\sigma E - \gamma I \tag{A.1d}$$

$$\frac{d}{dt}R = +\gamma I \tag{A.1e}$$

A.2 Incidence Rate

The incidence rate (force of infection) for non-vaccinated susceptible individuals in city c and risk group r ("group cr") is defined as:

$$\lambda_{cr} = \sum_{yc'r'} (1-\rho)\,\beta_y\,C_{ycr}\,\Phi_{ycrc'r'}\,\frac{I_{c'r'}}{N_{c'r'}} \tag{A.2}$$

where: ρ is the proportion isolating among infectious; β_y is the transmission probability per type-y contact; C_{ycr} is the type-y contact rate among group cr; $\Phi_{ycrc'r'}$ is the probability of type-y contact formation with group $c'r'$ among group cr; and N_{cr} is the size of group cr.

Among vaccinated, the incidence rate is simply reduced by a factor $(1-f)$, where f is the vaccine effectiveness (leaky-type).

A.3 Mixing

Mixing between risk groups and cities was implemented using an adaptation of a common approach [1,2]. We denote the total contacts "offered" by group cr as: $Q_{cr} = N_{cr}C_{cr}$; and denote the margins $Q_c = \sum_r Q_{cr}$; $Q_r = \sum_c Q_{cr}$; and $Q = \sum_{cr} Q_{cr}$. The probability of contact formation with group $c'r'$ among group cr is defined as:

$$\Phi_{crc'r'} = \epsilon_c\delta_{cc'}\left(\epsilon_r\delta_{rr'} + (1-\epsilon_r)\frac{Q_{c'r'}}{Q_{c'}}\right) + (1-\epsilon_c)\frac{Q_{c'}}{Q}\left(\epsilon_r\delta_{rr'} + (1-\epsilon_r)\frac{Q_{r'}}{Q}\right) \tag{A.3}$$

where: $\delta_{ii'} = \{1 \text{ if } i = i';\, 0 \text{ if } i \neq i'\}$ is an identity matrix; and $\epsilon_c, \epsilon_r \in [0,1]$ are assortativity parameters for mixing among cities and risk groups, respectively, such that $\epsilon = 1$ yields complete group separation and $\epsilon = 0$ yields completely random (proportionate) mixing. For clarity, we omit the index of contact type y, although ϵ_r, C_{cr} and thus $\Phi_{crc'r'}$ are all further stratified by y.

A.4 City R_0

The basic reproduction number R_0 for each city was defined in the absence of vaccination and ignoring between-city mixing — i.e. with $\epsilon_c = 1$. Following [3], we define R_0 as the dominant eigenvalue of the city-specific next generation matrix K; matrix elements $K_{rr'}$ are defined as:

$$K_{rr'} = (1-\rho)\sum_y \beta_y C_{yr}\Phi_{yrr'}\frac{N_r}{N_{r'}}\gamma^{-1} \tag{A.4}$$

where: ρ is the proportion isolating among infectious; β_y is the transmission probability per type-y contact; C_{yr} is the type-y contact rate among group r; $\Phi_{yrr'}$ is the probability of type-y contact formation with group r' among group r; N_r is the size of group r; and γ^{-1} is the duration of infectiousness.

A.5 Vaccine Allocation

Vaccination is modelled as distribution of 5000 doses over 15 days from day 60 (333 doses per day). Vaccines are prioritized to the high risk group with 90% sensitivity, such that 4500 doses actually reach the high risk group, and 500 doses are given to the lower risk group. Figure A.1 illustrates vaccination coverage/counts by city/risk group for an example allocation of 80% to city A and 20% to city B.

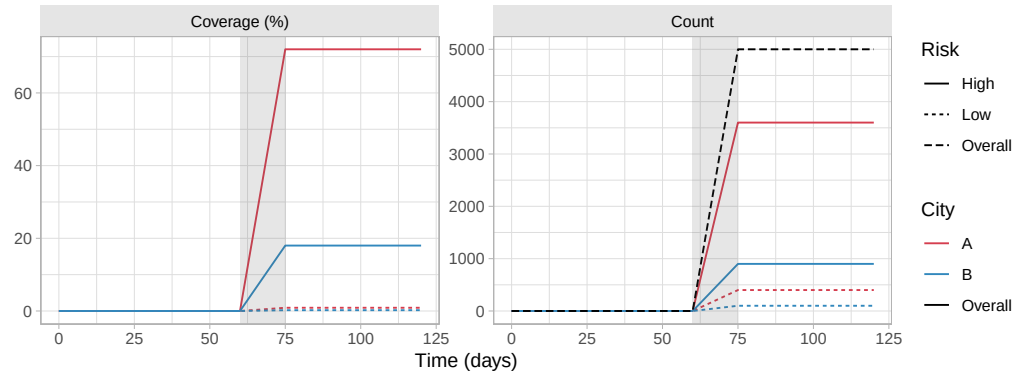

Figure A.1: Example vaccine allocation: 80% to city A, and 90% to high risk group

Gray bar indicates period of vaccine roll-out (days 60–75)

A.6 Parameterization

Model parameter values and stratifications are summarized in Table 1, repeated (verbatim) in Table A.2 for easier reference.

Sexual Behaviour: Parameterization of sexual behaviour was primarily informed by existing analyses conducted to support mathematical modelling of HIV-transmission among GBMSM in Canada [4, n.b. Appendix 3.2]. These analyses stratified GBMSM into 88–94% lower risk, with on average 4 sexual partners per-year ($\approx$ .01 per day), and 6–12% higher risk, with approximately 6-times as many partners ($\approx$ .07 per day). Our present model includes even greater partner numbers among the higher risk group (.10–.25 per day), partly to fit MPVX $R_0 \in [1, 2]$, and because the 6-fold value in [4] was mainly applied as a generalized proxy for 6-times higher HIV incidence. Weighted pooling of data from three studies [18–20] suggested that approximately 12% of respondents reported 20+ sexual partners in the past 6 months ($\approx$ .11+ per day). Our MPVX model also models transmission risk per-partnership, versus per-contact (sex act) as in [4]; with high SAR, MPVX transmission risk would be expected to be driven more by numbers of partners than by total contacts (sex acts).

Monkeypox Virus (MPVX): Updated epidemiological data on MPVX infection and transmission in the context of the present epidemic are rapidly emerging [9,21]. In the absence of high-quality evidence on the secondary attack rate (SAR) of sexual transmission, we assumed a relatively high SAR of 0.9 (per-partnership), drawing on local patient histories, and in order

Table A.2: Model parameters, including default values and ranges explored via grid sweep

Parameter	Stratum	Value	Range	Ref
Population size	overall	100,000		[4][a]
	fraction in city A	.50	[.20, .80]	[a]
Fraction higher risk	city A	.10	[.01, .50][b]	[4][a]
	city B	.10		[4][a]
Contact rate	close non-sexual, all	1		[a]
	sexual, low risk	.01		[4][a]
	sexual, high risk, city A	.178[c]	[.10, .25][b]	[4,5][a]
	sexual, high risk, city B	.178[c]		[4,5][a]
Assortativity	cities, all contacts	.90	[.70, 1.0]	[6][a]
	risk, close non-sexual	0		[a]
	risk, sexual	.50		[a]
Per-contact SAR	close non-sexual	.05		[7]
	sexual	.90[c]		[5][a]
Initial infections	overall	10		[a]
	fraction in city A	.50	[0.0, 1.0]	[a]
Duration of period	latent/incubation	7		[8–10]
	infectious/symptoms	21		[9,11]
Fraction isolated among infected		.50		[9][a]
Vaccines available		5000		[a]
Vaccine effectiveness[d]		.85		[12–14]
Vaccine prioritization sensitivity	high risk	.90		[15][a]
Vaccine allocation	city A	.50	[0.0, 1.0][e]	—

All durations in days; all rates in per-day. SAR: secondary attack rate. [a] Assumed / representative. [b] Calculated to fit $R_0 \in [1, 2]$. [c] Calculated to fit $R_0 = 1.5$, reflecting pre-vaccination estimate of MPVX R_0 in Ontario [16] via [17]. [d] Leaky-type. [e] Optimized parameter.

to reproduce $R_0 \in [1, 2]$. We estimated $R_0 \in [1, 2]$ using MPVX case data from Ontario [16] before widespread vaccine roll-out (2022 May 13 – July 4) using the `EpiNow2` R package [17].

In another model [5], the modelled R_0 for a GBMSM sexual network was greater, even for smaller SAR. Two main factors may explain this discrepancy in modelled R_0 vs SAR in [5] vs our model. First, isolation was not explicitly modelled in [5]; thus the reported SAR in [5] can be considered as after considering isolation, i.e., reduced. Second, the branching process model in [5] captured greater risk heterogeneity than our model, and focused especially on capturing the highest levels of risk ("heavy tail"). Such heterogeneity is directly related to R_0 through the coefficient of variation in contact rates [22]. Thus, this difference in model structure could further explain why modelled R_0 would be greater in [5], for even similar SAR. Finally, our aim was to obtain generalizable insights about network-level vaccine prioritization, rather than to model specific contexts within Ontario; as such, we do not expect our main findings to change with moderate changes to the model simplifications regarding transmission.

B Supplemental Results

Figure B.1 illustrates incidence rate and cumulative infections (similar results to Figure 2), for two cities identical in: size, R_0, and imported/seed cases, under three vaccination scenarios: no vaccination, 100% allocation to city A, and equal allocation between cities. Equal allocation minimizes cumulative infections.

Figures B.2–B.5 illustrate cumulative infections averted by day 120 under "optimal" vaccine allocation: versus no vaccination (absolute: B.2, relative: B.3), and versus allocation proportional to city size (absolute: B.4, relative: B.5).

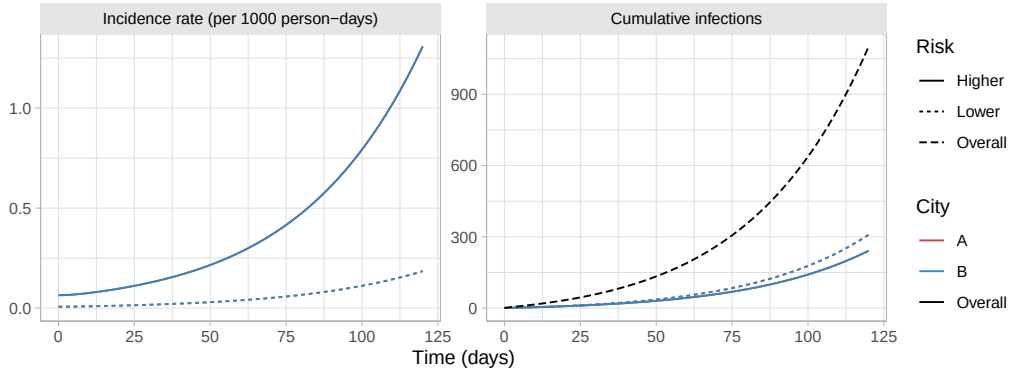

(a) No vaccination

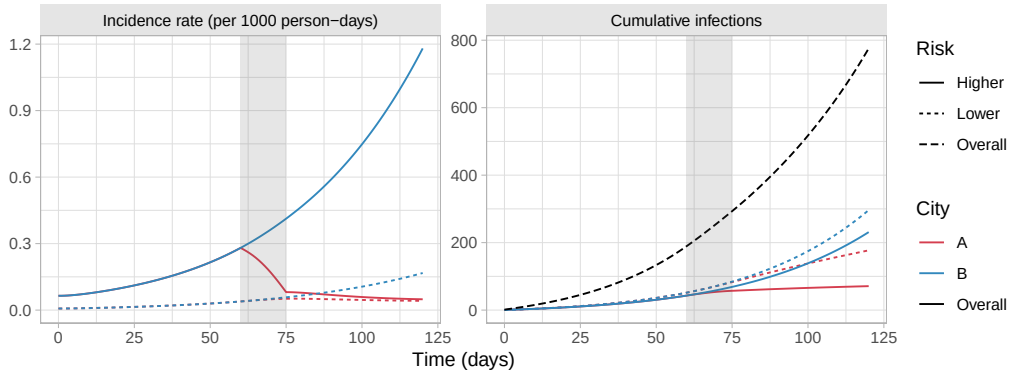

(b) 100% city A

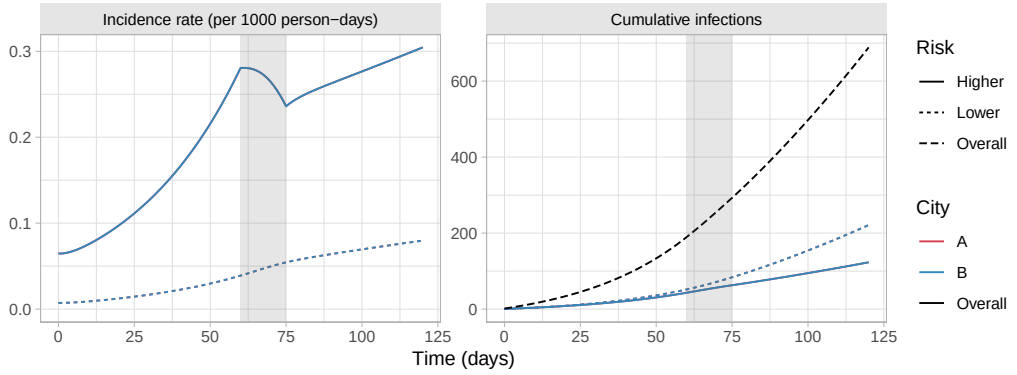

(c) Optimal: 50% city A, 50% city B

Figure B.1: Modelled monkeypox incidence and cumulative infections in cities A and B with default parameters, under two different vaccine allocation scenarios

Gray bar indicates period of vaccine roll-out (days 60–75).

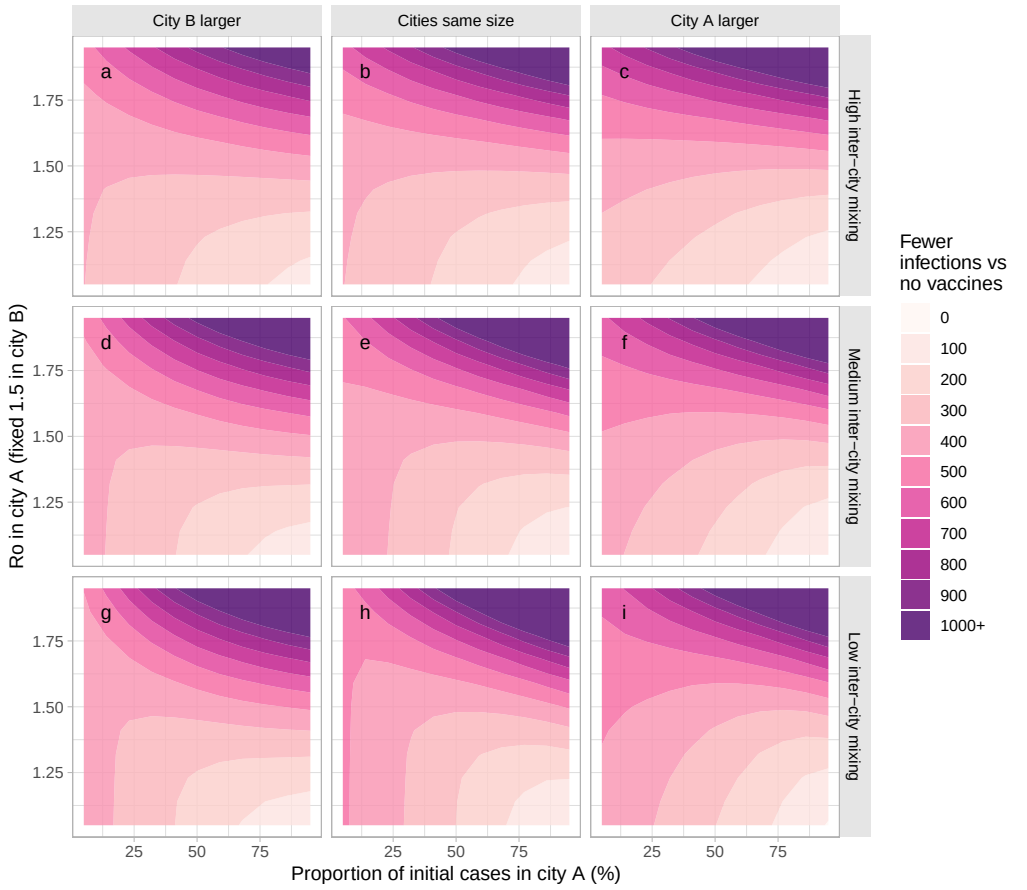

Figure B.2: Absolute fewer infections under optimal vaccine allocation versus no vaccination

R_0 in city A varies via the sexual activity among the high risk group in city A. Optimal allocation is defined as fewest cumulative infections by day 120. Larger city is 3 times the size of the other city. Most, moderate, and least inter-city mixing use $\epsilon_c = \{0.8, 0.9, 0.95\}$, respectively.

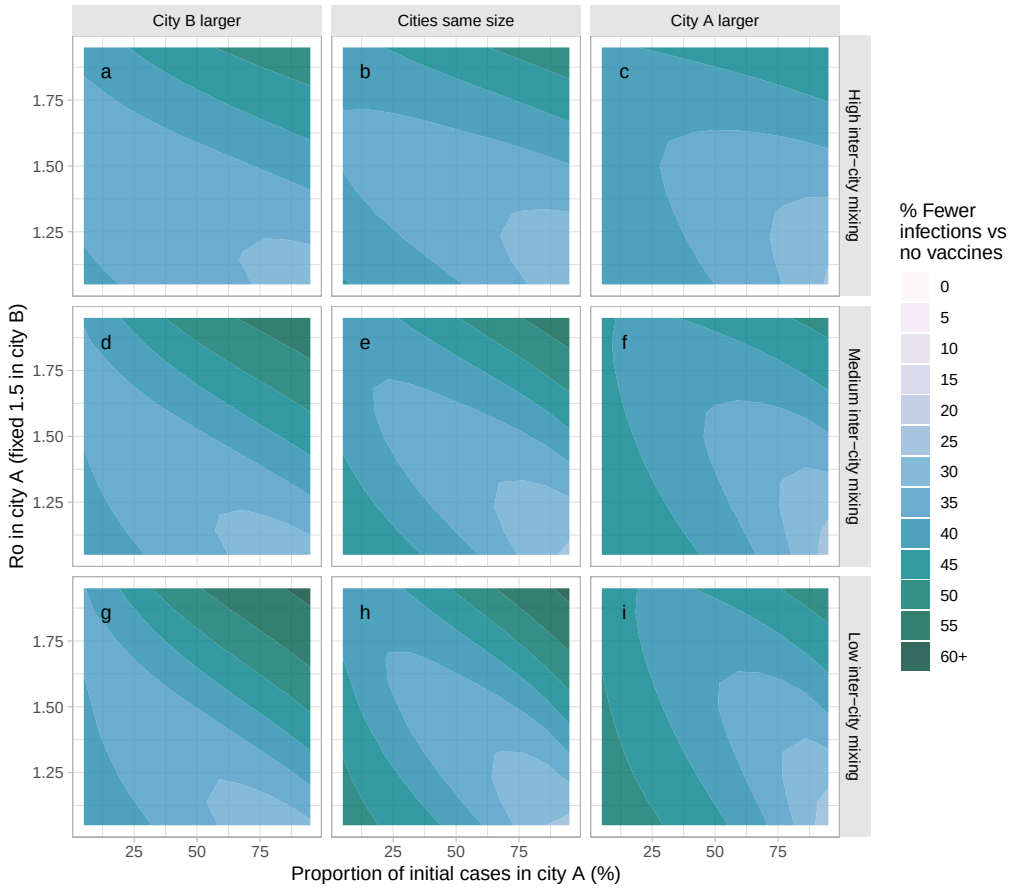

Figure B.3: Relative fewer infections under optimal vaccine allocation versus no vaccination

R_0 in city A varies via the sexual activity among the high risk group in city A. Optimal allocation is defined as fewest cumulative infections by day 120. Larger city is 3 times the size of the other city. Most, moderate, and least inter-city mixing use $\epsilon_c = \{0.8, 0.9, 0.95\}$, respectively.

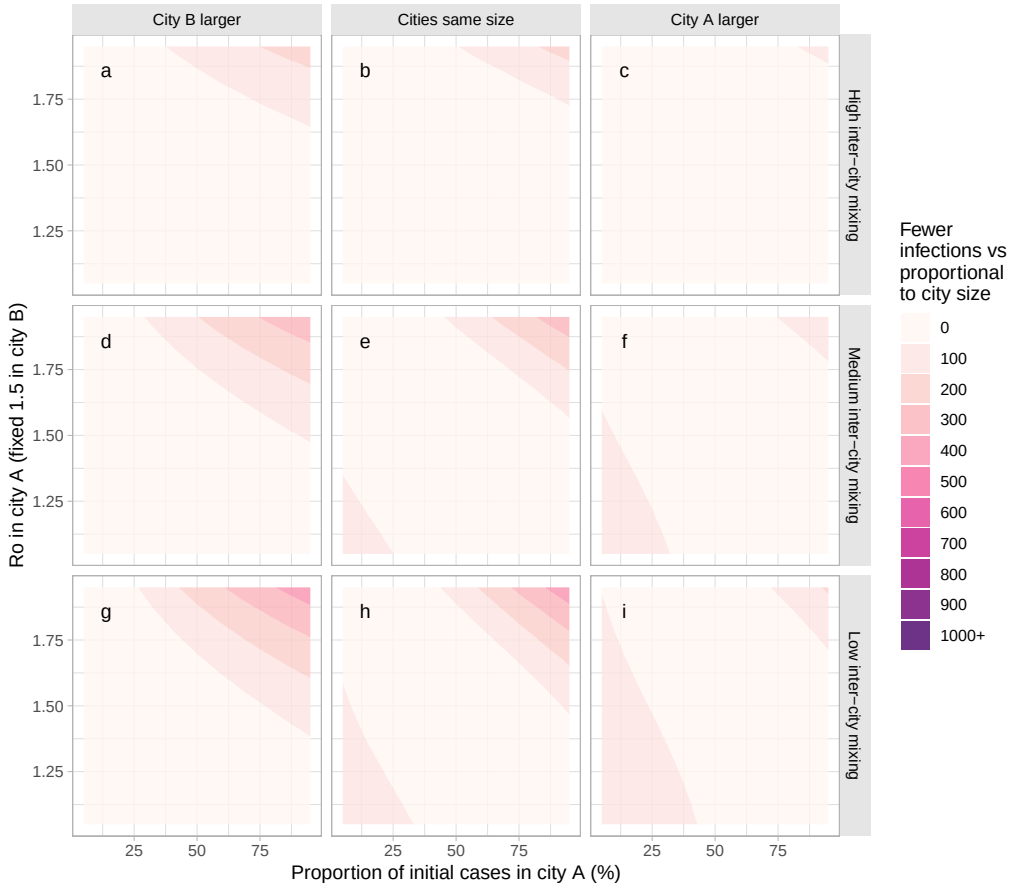

Figure B.4: Absolute fewer infections under optimal vaccine allocation versus allocation proportional to city size

R_0 in city A varies via the sexual activity among the high risk group in city A. Optimal allocation is defined as fewest cumulative infections by day 120. Larger city is 3 times the size of the other city. Most, moderate, and least inter-city mixing use $\epsilon_c = \{0.8, 0.9, 0.95\}$, respectively.

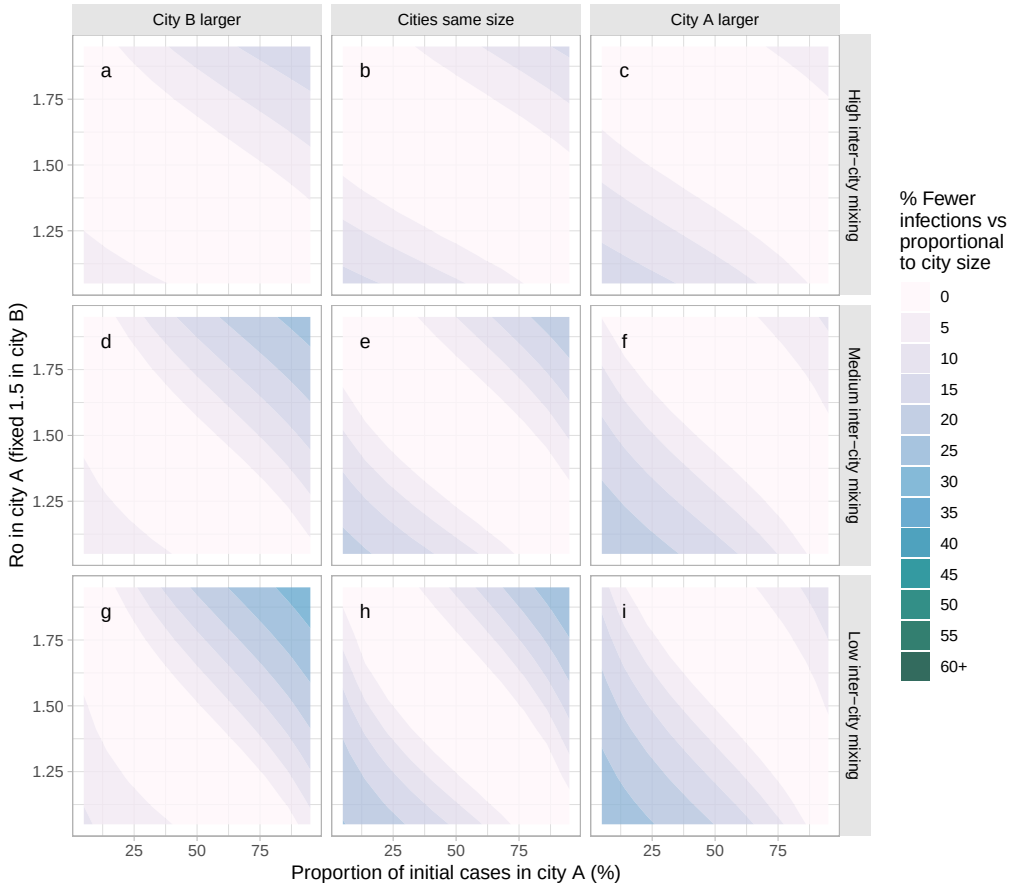

Figure B.5: Relative fewer infections under optimal vaccine allocation versus allocation proportional to city size

R_0 in city A varies via the sexual activity among the high risk group in city A. Optimal allocation is defined as fewest cumulative infections by day 120. Larger city is 3 times the size of the other city. Most, moderate, and least inter-city mixing use $\epsilon_c = \{0.8, 0.9, 0.95\}$, respectively.

References

[1] Annett Nold. "Heterogeneity in disease-transmission modeling". In: *Mathematical Biosciences* 52.3-4 (Dec. 1980), pp. 227–240. URL: http://www.doi.org/10.1016/0025-5564(80)90069-3.

[2] Geoffrey P. Garnett and Roy M. Anderson. "Balancing sexual partnerships in an age and activity stratified model of HIV transmission in heterosexual populations". In: *Mathematical Medicine and Biology* 11.3 (Jan. 1994), pp. 161–192. URL: http://www.doi.org/10.1093/imammb/11.3.161.

[3] O. Diekmann, J. A.P. Heesterbeek, and J. A.J. Metz. "On the definition and the computation of the basic reproduction ratio Ro in models for infectious diseases in heterogeneous populations". In: *Journal of Mathematical Biology* 28.4 (1990), pp. 365–382. URL: http://www.doi.org/10.1007/BF00178324.

[4] Linwei Wang et al. "Mathematical modelling of the influence of serosorting on the population-level HIV transmission impact of pre-exposure prophylaxis". In: *AIDS* 35.7 (June 2021), pp. 1113–1125. URL: http://www.doi.org/10.1097/QAD.0000000000002826.

[5] Akira Endo et al. "Heavy-tailed sexual contact networks and the epidemiology of monkeypox outbreak in non-endemic regions, May 2022". In: *medRxiv* (June 2022). URL: https://doi.org/10.1101/2022.06.13.22276353.

[6] Eric Armstrong et al. "Travelling for sex, attending gay-specific venues, and HIV-related sexual risk among men who have sex with men in Ontario, Canada". In: *Canadian Journal of Human Sexuality* 29.3 (Dec. 2020), pp. 380–391. URL: http://www.doi.org/10.3138/CJHS.2019-0054.

[7] Ellen M. Beer and V. Bhargavi Rao. "A systematic review of the epidemiology of human monkeypox outbreaks and implications for outbreak strategy". In: *PLOS Neglected Tropical Diseases* 13.10 (2019), e0007791. URL: http://www.doi.org/10.1371/journal.pntd.0007791.

[8] Kelly Charniga et al. "Estimating the incubation period of monkeypox virus during the 2022 multi-national outbreak". In: *medRxiv* (June 2022). URL: http://www.doi.org/10.1101/2022.06.22.22276713.

[9] John P. Thornhill et al. "Monkeypox Virus Infection in Humans across 16 Countries - April-June 2022". In: *New England Journal of Medicine* (July 2022). URL: https://doi.org/10.1056/NEJMoa2207323.

[10] Fuminari Miura et al. "Estimated incubation period for monkeypox cases confirmed in the Netherlands, May 2022". In: *Eurosurveillance* 27.24 (June 2022). URL: http://www.doi.org/10.2807/1560-7917.es.2022.27.24.2200448.

[11] Hugh Adler et al. "Clinical features and management of human monkeypox: a retrospective observational study in the UK". In: *The Lancet Infectious Diseases* 22.8 (Aug. 2022), pp. 1153–1162. URL: http://www.doi.org/10.1016/s1473-3099(22)00228-6.

[12] P. E.M. Fine et al. "The transmission potential of monkeypox virus in human populations". In: *International Journal of Epidemiology* 17.3 (Sept. 1988), pp. 643–650. URL: https://doi.org/10.1093/ije/17.3.643.

[13] Public Health Agency of Canada. *Interim guidance on the use of Imvamune in the context of monkeypox outbreaks in Canada*. June 2022. URL: https://www.canada.ca/content/dam/phac-aspc/documents/services/immunization/national-advisory-committee-on-immunization-naci/guidance-imvamune-monkeypox/guidance-imvamune-monkeypox-en.pdf.

[14] United States Centers for Disease Control and Prevention. *Monkeypox and Smallpox Vaccine Guidance*. June 2022. URL: https://www.cdc.gov/poxvirus/monkeypox/clinicians/smallpox-vaccine.html.

[15] Toronto Public Health. *Monkeypox Vaccine Fact Sheet*. Aug. 2022. URL: https://www.toronto.ca/wp-content/uploads/2022/07/97ef-MonkeypoxVaccineFactSheet.pdf.

[16] Public Health Ontario. *Monkeypox in Ontario: May 20, 2022 to August 15, 2022*. Aug. 2022. URL: https://www.publichealthontario.ca/en/Diseases-and-Conditions/Infectious-Diseases/Vector-Borne-Zoonotic-Diseases/Monkeypox.

[17] Sam Abbott et al. *EpiNow2: Estimate Real-Time Case Counts and Time-Varying Epidemiological Parameters*. 2020. URL: http://www.doi.org/10.5281/zenodo.3957489.

[18] Ted Myers et al. *Male Call Canada Technical Report*. 2013. URL: https://web.archive.org/web/20180203015550/http://www.malecall.ca/technical-report/.

[19] Nathan J. Lachowsky et al. "Pre-exposure Prophylaxis Awareness Among Gay and Other Men who have Sex with Men in Vancouver, British Columbia, Canada". In: *AIDS and Behavior* 20.7 (July 2016), pp. 1408–1422. URL: http://www.doi.org/10.1007/s10461-016-1319-8.

[20] James Wilton et al. “Use of an HIV-risk screening tool to identify optimal candidates for PrEP scale-up among men who have sex with men in Toronto, Canada: Disconnect between objective and subjective HIV risk”. In: *Journal of the International AIDS Society* 19.1 (Jan. 2016), p. 20777. URL: http://www.doi.org/10.7448/IAS.19.1.20777.

[21] Public Health Ontario. *Multi-Jurisdictional Monkeypox Outbreak 2022 – What We Know So Far*. July 2022. URL: https://www.publichealthontario.ca/en/Diseases-and-Conditions/Infectious-Diseases/Vector-Borne-Zoonotic-Diseases/Monkeypox.

[22] R. M. Anderson et al. “A preliminary study of the transmission dynamics of the Human Immunodeficiency Virus (HIV), the causative agent of AIDS”. In: *Mathematical Medicine and Biology* 3.4 (Jan. 1986), pp. 229–263. URL: http://www.doi.org/10.1093/imammb/3.4.229.